Acta Cryst. (1994). D**50**, 276–282

Data Collection at Short Wavelengths in Protein Crystallography

BY A. GONZALEZ

SERC Daresbury Laboratory, Warrington WA4 4AD, England

R. DENNY

Physics Department, Imperial College, London SW7 2BZ, England

AND C. NAVE

SERC Daresbury Laboratory, Warrington WA4 4AD, England

(*Received* 1 *June* 1993; *accepted* 23 *November* 1993)

Abstract

The development of high-intensity X-ray sources and the use of insertion devices will make it possible to collect data routinely from protein crystals at very short wavelengths ($\lambda \leq 0.5$ Å). Possible benefits of using shorter wavelengths can be inferred from the improvement in the quality of the data when using a wavelength $\lambda \simeq 0.9$ Å instead of one close to the Cu $K\alpha$ emission edge. In addition to fewer absorption errors, two factors might contribute to this improvement. These are an increase in the lifetime of the protein crystal and a better signal-to-background ratio. In this paper we address the second of these. In order to compare the quality of the data and the relative background level in the diffraction patterns at different wavelengths two data sets have been collected at $\lambda = 0.92$ and 0.55 Å. The results obtained from data processing and careful measurement of the background in the raw images suggest that, in the absence of absorption errors and radiation damage, data collection at very short wavelengths does not provide higher quality data. There is no improvement in the signal-to-background ratio in the short-wavelength data.

1. Introduction

The benefits of using short X-ray wavelengths to collect protein crystal data have been discussed by Helliwell, Ealick, Doing, Irving & Szebenyi (1993). Potential benefits include a reduction in absorption errors, a decrease in radiation damage and an improvement in the signal-to-background ratio. Unfortunately, there has been a lack of systematic experimental studies to determine to what extent these claims are correct, probably because of the lack of X-ray sources providing high intensities and the lower sensitivity of many detectors at shorter wavelengths. There is much anecdotal evidence concerning the better quality of data collected near 0.9 Å compared to 1.5 Å. Nevertheless it is not known whether this is a general result or if it can be extrapolated to the short wavelengths available from high-energy synchrotron sources.

Most of the processes taking place when the X-rays interact with the sample (heating, photoelectric absorption, Compton scattering) are likely to cause direct or indirect radiation damage in the crystal and an increase in the background of the pattern, either directly or as a result of radiation damage. All the processes mentioned above are linked to the flux absorbed by the crystal, which, in general, decreases at shorter wavelengths. However, the elastic scattering also decreases with the wavelength. The integrated intensity of a crystal diffraction spot for small Bragg angles is

$$I \propto \delta^3 \lambda^2 \exp(-\mu\delta), \qquad (1)$$

where δ is the dimension of the crystal, λ is the wavelength and μ is the absorption coefficient. Arndt (1984) has pointed out that one of the aims when choosing the wavelength is to maximize the diffracted intensity for a given X-ray dose deposited in the specimen. It is not certain whether radiation damage is likely to follow the energy absorbed or quanta absorbed. If the former is the relevant factor, there would be no advantage in collecting data at short wavelengths to minimize the radiation damage. When the transmission through the crystal is high the energy absorbed per scattered photon is practically independent of the wavelength [see Fig. 1 in Arndt (1984)]. Radiation damage is dependent on many factors (*e.g.* sample, temperature, data-collection time) in addition to the wavelength used. In this paper we address the question of the signal-to-background ratio at different wavelengths without considering radiation damage. A different protocol is required to study radiation damage and such experiments will be described in a later paper.

ISSN 0907-4449

Helliwell *et al.* (1993) have argued that the background on a diffraction image (with the exception of the background arising from elastic scattering) falls off as l^2, where l is the sample-to-detector distance; therefore, an improvement can be achieved at shorter wavelengths as it is possible to move the detector further away from the sample and get the same resolution at the edge of the detector. This requires that the Bragg spots remain sharp as the distance is increased. Some of the factors whose contribution to the signal-to-background ratio depends on the wavelength are:

(1) Background arising from elastic scattering from liquid around the crystal, disordered solvent in the crystal, capillary tube, *etc.*

(2) Heat-induced disorder and thermal parameters.

(3) Background caused by inelastic scattering and fluorescence.

(4) Efficiency of the detector if different wavelengths are present in the signal and the background.

Clearly, a theory-based estimation of the optimum wavelength for monochromatic experiments is difficult, given the great number of factors to be considered. The experiment described below was designed to provide a relatively unbiased estimate of the effect of some of these factors on the signal-to-background ratio at two different wavelengths. In addition, the quality of the data at the two wavelengths is compared.

2. Methods

2.1. *Experimental set-up*

The sample chosen was a HEW (hen egg white) lysozyme tetragonal crystal (space group $P4_32_12$). These crystals are easily grown to a good size (0.3–0.5 mm), diffract very well to a resolution well above 1.8 Å and are reasonably stable in an X-ray beam. The data collection was carried out on the SRS wiggler station 9.5 (Thompson *et al.*, 1992). A wide range of wavelengths are available by rotating the double-crystal monochromator. We selected the wavelengths 0.92 and 0.55 Å, the former representing wavelengths commonly used for routine data collection at many synchrotron sources and the latter as a wavelength for which fast data collection can be available at higher intensity sources. At both these wavelengths absorption errors are small. We collected data with a 90 mm radius MAR image plate. The efficiency of a detector as a function of the wavelength depends mainly on the absorption efficiency of the phosphor compound in image plates and TV detectors, silver bromide in films and the gas in gas-filled detectors. From this point of view, an image plate is perhaps the best detector available to collect data at short wavelengths. The absorption of film falls quite rapidly below the bromide edge at 0.92 Å, while the absorption of 0.15 mm thick BaFBr phosphor at 0.55 Å is only about 20% less than that at 0.92 Å (Amemiya, 1990).

Table 1. *Data-collection parameters at wavelengths* 0.55 *and* 0.92 Å

The average intensity, number of reflections and overall R factor are given for the two independently scaled data sets after Lorentz and polarization corrections were applied in *DENZO*.

	Data-collection wavelength	
	λ = 0.92 Å	λ = 0.55 Å
Sample-to-detector distance (mm)	146.65	258.79
Oscillation range ( )	9	9
Exposure time (s deg $^{-1}$)	20	150
Maximum resolution (Å)	1.8	1.8
Completeness (%)	45	45
Overall R factor	0.073	0.072

We tried to make the experimental conditions at both wavelengths as similar as possible. We used the same crystal in the same real-space orientation with respect to the beam to minimize changes caused by different size and anisotropy in the crystal and to obtain a large number of equivalent reflections common to both data sets. The detector was moved closer to the protein crystal for the collection at 0.92 Å to obtain approximately the same data resolution at the detector edge and the exposure time shortened so that the detector was similarly exposed at both wavelengths (see Table 1). We collected oscillation data at 0.55 Å first and then at 0.92 Å over a total oscillation range of 9° with an oscillation of 1.5° in each image. There was a dead time between exposures of about 2 min while the image plate was scanned. With the short oscillation range the crystal does not deteriorate significantly in the beam and the data set is complete enough to obtain reliable statistics.

2.2. *Data analysis*

In order to compare the quality of the data at the two wavelengths, both data sets were processed independently with the program package *DENZO* (Otwinowski, 1991). Reflections from individual images were scaled and merged with the *CCP*4 programs *ROTAVATA* and *AGROVATA* (*CCP*4 suite, SERC Daresbury Laboratory, 1979). The Lorentz and polarization corrections were applied to the data for this comparison.

2.3. *Signal-to-background measurement*

The background level was measured directly from the diffraction patterns and corrected by subtracting the 'dark signal' of the detector, found to be ~8 by reading the image scanner without X-ray exposure. The program *DENZO*, like many other data-

processing programs, applies a series of corrections to the output intensities (*i.e.* polarization, Lorentz, air absorption, *etc.*) The exact Lorentz correction depends much on the geometry of the problem, but the wavelength dependence is approximately λ^{-1}. This particular term of the intensity-correction factor is going to inflate the processed spot intensities from the short-wavelength data set with respect to that obtained using long wavelengths. The polarization, in comparison, constitutes a much smaller correction. To compare the actual background intensity recorded on the detector we reprocessed the images removing the Lorentz and polarization contributions to the intensity-correction factor. We used two different scales:

(1) The scale factor between individual images (n and m) in each data set. This scale factor, $I^n_{0.55}/I^m_{0.92}$, was calculated with the program *ROTAVATA* by merging the intensities from all the images in both data sets.

(2) The ratio between the profile-fitted raw intensities of an individual reflection collected with both wavelengths, $I^{(h,k,l)}_{0.55}/I^{(h,k,l)}_{0.92}$.

To obtain an initial estimate of the background level in the first pattern of each data set the scaling factor $I^n_{0.55}/I^m_{0.92}$ between the images was calculated and applied to the background, at about 7 Å resolution, away from Bragg spots (shown in Fig. 1). The background was also compared around individual spots using either the scale between the images at the different wavelengths, $I^n_{0.55}/I^m_{0.92}$, or the measured intensity of the reflection, $I^{(h,k,l)}_{0.55}/I^{(h,k,l)}_{0.92}$. Finally, the background was extracted from each data set by locally rejecting outliers (diffraction spots) from small overlapping regions of the pattern using the program *LSQINT* (R. Denny, in preparation). The dark signal was subtracted from the total background and the background images were then scaled by $I^1_{0.55}/I^1_{0.92} = 1.6$ and circularly averaged using the programs *BSL* (Bordas & Mant, unpublished work) and *OTOKO* (Koch, Bendall, Bordas & Mant, unpublished work).

2.4. *Precision of the comparison*

It is not possible to compensate exactly for a change in wavelength by moving the detector to a different distance. This is because, with a flat detector, different parts of the detector are further away from the sample. This effect is proportionally greater for the long-wavelength data. In this experiment, the distances were set to compensate for the wavelength change at one radius on the detector. The assumption that the wavelength-dependent term in

Zms - \/Yms	734	735	736	737	738	739	740	741	742	743	744
615:	43	42	52	57	59	40	40	42	48	54	54
614:	43	45	51	51	59	50	45	34	45	49	50
613:	50	55	54	59	46	45	55	56	59	58	53
612:	51	56	48	45	40	42	47	51	49	55	57
611:	53	46	47	41	45	47	64	58	56	56	53
610:	46	38	43	40	44	54	60	59	71	60	56
609:	41	56	59	49	42	46	48	66	73	57	54
608:	46	55	58	61	54	51	46	58	62	51	48
607:	51	58	53	61	64	58	51	44	55	51	45
606:	45	50	61	59	52	42	39	47	56	56	55
605: /\Yms	47	40	43	48	49	45	42	39	45	56	55
Zms -	734	735	736	737	738	739	740	741	742	743	744

Zms - \/Yms	721	722	723	724	725	726	727	728	729	730	731
620:	29	28	37	31	26	30	28	33	32	27	37
619:	37	32	31	33	30	32	33	35	28	32	38
618:	41	43	28	28	30	34	35	30	28	35	44
617:	43	34	22	19	21	31	42	34	33	40	39
616:	38	34	23	25	21	27	33	36	43	40	37
615:	35	33	28	29	27	33	30	51	36	33	34
614:	36	30	29	34	28	37	35	35	36	38	30
613:	30	37	33	48	35	20	21	16	30	37	29
612:	42	35	39	42	45	31	23	26	32	33	37
611:	39	32	37	37	43	39	31	31	32	31	33
610: /\Yms	38	38	29	27	31	30	30	32	38	35	30
Zms -	721	722	723	724	725	726	727	728	729	730	731

Fig. 1. Comparison of the background in the first image of two data sets collected at different wavelengths. At $\lambda = 0.55$ Å (top) the average background after subtracting the dark current contribution is near 42. At $\lambda = 0.92$ Å (bottom) the figure is around 26. Multiplication of this figure by the scale factor between the images $I^1_{0.55}/I^1_{0.92} = 1.6$, we obtain the approximate value of 43 for the background level in the bottom profile.

the Lorentz factor varies as λ^{-1} is also only approximate. This means that the scale factor for the spot intensities on the image, $I_{0.55}^{(h,k,l)}/I_{0.92}^{(h,k,l)}$, will vary across the image. In addition, the actual data (diffraction spots and background) obtained at the two wavelengths is different due to the different curvature of the spheres of reflection. The overall data quality also depends on the exposure time. Obtaining the relative exposure from the intensities on the image is complicated by the fact that the response of the image plate varies with wavelength. The experiment was designed to give average estimates of the signal-to-background ratio and data quality on the raw image under normal experimental conditions. Some information concerning the above points is also obtained.

3. Results

3.1. *Overall data quality*

The merging R factors for the intensities were 0.072 for 3495 reflections from the $\lambda = 0.55$ Å data set and 0.073 for 4103 reflections for the $\lambda = 0.92$ Å data. Table 2 shows that the R factors and $I/\sigma(I)$ as a function of resolution and intensity are similar. Slightly better statistics are obtained for the long-wavelength data set. As a result of the increased curvature of the sphere of reflection, a greater number of reflections (mainly at high resolution) are available for scaling at long wavelength. The increased number of these weak reflections means that the overall R factor is slightly worse.

The statistics obtained for each data set are very similar, despite the higher signal at the shorter wavelength (compare the intensities in Figs. 2 and 3). An explanation for this is the different response of the detector per absorbed photon in the image plate. The signal for a photon absorbed at $\lambda = 0.55$ Å is approximately 1.45 times that for a photon absorbed at 0.92 Å [Fig. 1 of Ito & Amemiya (1991)]. This is close to the scale obtained between the data sets at the two wavelengths in this study. Despite the different signal in the images, the number of photons absorbed by the plate would then be similar and so are the statistics.

3.2. *Signal-to-background estimation*

The background ratio between the two initial patterns in each data set after the images were scaled together was $B_{0.55}^1/B_{0.92}^1 = 0.98$ (Fig. 1). Fig. 2 shows the profile of the reflection $h,k,l = 2,4,-3$ and the surrounding background. The scale between the two images where this particular reflection was recorded is $I_{0.55}^1/I_{0.92}^2 = 2.1$. A similar estimate can be obtained from the intensities of the 2,4,−3 reflection. From these the scale $I_{0.55}^{(2,4,-3)}/I_{0.92}^{(2,4,-3)}$ is 2.0. Applying these scales the background-level ratio, $B_{0.55}^1/B_{0.92}^2$, was between 0.79 and 0.82. The profile of a higher resolution reflection as $h,k,l = 0,19,17$ is shown in Fig. 3. *ROTAVATA* gives a scale $I_{0.55}^5/I_{0.92}^1$ between the images of 1.4, while $I_{0.55}^{(0,19,17)}/I_{0.92}^{(0,19,17)}$ is 1.5. Depending on which scale is applied $B_{0.55}^5/B_{0.92}^1$ varies between 1.15 and 1.19.

Table 2. *Data analysis against resolution*

R factor, average intensity, intensity/σ ratio, number of measured reflections and number used in the scaling in each resolution bin for (*a*) 0.55 Å data and (*b*) 0.92 Å data. Note that the intensity values correspond to processed data for which a Lorentz correction has been applied.

(*a*) 0.55 Å

d(Å)	R	I	I/σ	N_{scale}
3.91	0.035	2662	17.0	405
2.82	0.049	1193	13.3	700
2.31	0.105	459	6.6	879
2.01	0.173	276	4.4	860
1.80	0.378	113	2.0	651

(*b*) 0.92 Å

d(Å)	R	I	I/σ	N_{scale}
3.91	0.028	2314	22.6	410
2.82	0.043	1333	15.9	745
2.31	0.103	520	6.7	917
2.01	0.169	276	4.4	1065
1.80	0.325	129	2.3	966

The radial variation of the background on the first image of each data set is shown in Fig. 4. The background level is not constant throughout the pattern. It increases sharply between 5 and 2.5 Å because of diffraction by non-protein material (capillary tube and mother liquor) and disorder in the crystal. The backgrounds are equal at approximately 35 mm from the centre of the plate. Near the centre of the plate, away from the beamstop region, the signal-to-background ratio is approximately 7% lower for the short-wavelength data set. An 11% lower background would be expected precisely at the centre of the plate for the distances and wavelengths used. At the edge of the plate the short-wavelength data have about a 30% higher background. However, the distribution of background intensity in reciprocal space is not uniform. The only point, apart from the origin, where the backgrounds can be directly compared with the changes expected due to the different distances and angles of incidence on the plate is at 70 mm from the centre. Here, the reciprocal spacings from the two images are approximately equal. At this radius, the ratio of short-wavelength to long-wavelength background is approximately 1.25. Taking into account the different distances and angles of incidence at this point, a ratio of 1.10 is predicted. The most likely reason for the discrepancy is that different amounts of the crystal and the disordered material were illuminated at the two wavelengths. The differences between the background curves are consistent with this.

2ms - \/Yms	566	567	568	569	570	571	572	573	574	575	576
687:	34	45	35	33	50	50	43	49	53	60	51
686:	40	39	46	49	45	38	46	46	52	43	42
685:	44	48	53	76	94	92	122	95	75	58	42
684:	40	43	82	206	380	483	539	273	112	63	49
683:	48	61	154	847	2449	2720	1836	697	175	75	56
682:	67	71	343	2246	5839	7735	3909	862	155	59	49
681:	46	89	366	1922	3994	3182	1366	436	86	42	40
680:	56	50	81	199	576	560	187	115	56	46	48
679:	53	55	57	44	65	79	54	50	43	39	49
678:	45	50	49	45	42	46	39	44	50	53	55
677:	46	46	43	50	47	49	55	52	46	42	46
/\Yms											
2ms -	566	567	568	569	570	571	572	573	574	575	576

2ms - \/Yms	568	569	570	571	572	573	574	575	576	577	578
683:	20	39	33	29	21	29	28	31	33	32	32
682:	28	48	41	28	25	34	39	33	38	31	31
681:	38	46	44	43	66	88	73	57	46	27	27
680:	37	36	50	86	267	414	290	132	65	40	32
679:	39	44	100	438	1236	1968	1194	352	83	41	34
678:	35	46	176	1294	3900	3925	1624	317	63	40	42
677:	28	46	150	704	2318	2640	952	120	37	34	31
676:	34	39	48	139	231	301	167	55	34	25	29
675:	41	35	27	31	47	49	46	36	30	27	30
674:	36	34	32	25	29	37	36	33	24	31	37
673:	33	30	24	29	47	47	27	34	25	33	35
/\Yms											
2ms -	568	569	570	571	572	573	574	575	576	577	578

Fig. 2. Randomly chosen 10.8 Å reflection $h,k,l = 2,4,-3$ collected both with a short wavelength $\lambda = 0.55$ Å (top profile) and with the longer wavelength $\lambda = 0.92$ Å (bottom). The scale $I^2_{0.55}/I^1_{0.92}$ is 2.1 and the ratio of the raw intensities $I^{(2,4,-3)}_{0.55}/I^{(2,4,-3)}_{0.92}$ is 2.03. Applying either scale to the average background intensity of the $\lambda = 0.92$ Å reflection gives a value close to 50. In the case of the $\lambda = 0.55$ Å reflection the background is near 40.

2ms - \/Yms	852	853	854	855	856	857	858	859	860	861	862
183:	69	72	68	69	83	82	74	68	60	56	70
182:	62	72	72	69	71	55	62	55	57	57	69
181:	67	56	53	56	55	56	67	74	65	60	72
180:	46	44	58	70	72	74	78	90	83	72	71
179:	63	53	57	73	106	118	124	103	97	79	72
178:	66	63	81	72	100	130	125	104	96	77	68
177:	76	75	74	76	84	121	108	103	86	72	72
176:	70	72	62	67	79	80	96	83	77	67	53
175:	69	66	68	79	85	118	108	89	74	74	54
174:	69	79	83	85	79	84	93	82	67	79	72
173:	71	77	81	71	58	62	70	71	70	64	80
/\Yms											
2ms -	852	853	854	855	856	857	858	859	860	861	862

2ms - \/Yms	857	858	859	860	861	862	863	864	865	866	867
181:	39	39	38	40	47	41	48	37	42	46	39
180:	42	38	43	47	62	57	51	38	39	49	47
179:	41	41	55	77	79	66	51	44	41	39	38
178:	42	41	52	78	82	69	55	41	42	41	40
177:	41	50	51	61	73	75	64	40	37	41	32
176:	42	43	42	44	63	84	72	40	34	36	35
175:	40	37	29	40	72	88	78	42	35	31	33
174:	43	37	32	41	56	62	53	41	38	40	37
173:	35	33	33	40	47	54	40	35	32	35	34
172:	31	40	45	42	42	53	40	31	28	34	33
171:	36	40	43	42	34	26	31	19	27	27	28
/\Yms											
2ms -	857	858	859	860	861	862	863	864	865	866	867

Fig. 3. Random 1.9 Å reflection $h,k,l = 0,17,19$ and a symmetry equivalent collected with $\lambda = 0.55$ Å (top profile) and $\lambda = 0.92$ Å (bottom profile). The scale between the images is $I^5_{0.55}/I^1_{0.92} = 1.4$. Corrected by this value, the average background level with $\lambda = 0.92$ Å is approximately 51, compared with a value of 61 for the $\lambda = 0.55$ Å image. If the scaling is based on the ratio of the raw intensities of the particular reflection $I^{(0,17,19)}_{0.55}/I^{(0,17,19)}_{0.92} = 1.5$ a background level of 54 is obtained for the $\lambda = 0.92$ Å reflection.

Although an increase in the spot size might be expected at the shorter wavelength because of the bigger distance between the sample and the detector, in practice this is unnoticeable because of the low divergence of the synchrotron source, in this case 1 mrad horizontally by 0.1 mrad vertically.

4. Discussion

The results of this experiment seem to prove that data collected from a typical protein crystal with $\lambda = 0.55$ and $\lambda = 0.92$ Å do not show a significant difference either in the spot-to-background intensity or in overall data quality. One can use the results above to understand how the various factors enumerated in the *Introduction* contribute.

4.1. *Radiation damage*

There is no evidence from our data that crystal deterioration as a result of radiation damage took place during the experiment. Note that any slight increase in the background level as a result of radiation damage should affect the longer wavelength data, since they were collected last.

4.2. *Detector efficiency*

For image plates, the detector response per absorbed photon and per incident photon have been documented by Ito & Amemiya (1991). The main concern for data collection is the statistics obtained per incident photon. The results obtained here appear to demonstrate a difference in the statistics for a given signal at different wavelengths, consistent with the data given by Ito & Amemiya (1991).

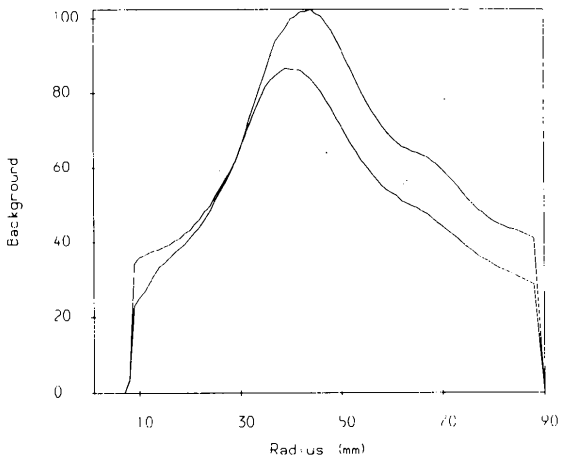

Fig. 4. Radially averaged background (determined as described in the text) as a function of radius on the detector for the short-wavelength data (top curve) and the long-wavelength data (bottom curve).

However, the response of the image plate also depends on the readout system. At higher energies, the photons absorbed will create deeper traps in the phosphor and these could take a longer time to read out with a laser.

4.3. *Background caused by non-crystalline elastic scattering*

This type of scattering obeys Bragg's equation, that is to say, its contribution to the background will concentrate at smaller angles as the wavelength is reduced. We did not get a reduction in the background by moving back the detector to compensate for the change in wavelength. This is consistent with non-crystalline elastic scattering being the main contributor to the total background at the wavelengths used in the experiment.

4.4. *Thermal disorder*

The energy per second dissipated as heat in a small crystal can be approximated as (see Helliwell, 1992),

$$dE/dt \propto \delta^3 \lambda^2, \qquad (2)$$

where δ is the linear dimension of the crystal. From (2) one can see that the use of a small wavelength can reduce the amount of heat absorbed by the specimen and possibly the amount of disorder caused by thermal vibrations. If this is the case, high-resolution reflections obtained with small wavelengths could be more intense. However, the scattered intensity also varies as λ^2 [see (1)]. Although the heat absorbed per second by the crystal is less at 0.55 Å, the necessary increase in exposure time at this wavelength makes the total absorbed heat practically independent of the wavelength, since both diffracted intensity and heat absorption vary as $\sim\lambda^2$. The temperature rise expected at 0.92 Å is, in any case, less than 0.03 K s^{-1}, assuming adiabatic conditions. It is therefore unlikely that a significant increase in temperature would occur with the exposure time of 30 s per image used in the experiment. Thus one cannot expect a decrease of the intensity of a reflection, owing to increased temperature factors, at the longer wavelength with the intensities used here.

4.5. *Other processes*

The atomic cross section for photoelectric absorption depends on the atomic number Z as Z^5 (Christy & Pytte, 1965) and it can be high near heavy-atom absorption edges; in this case it would be advantageous to increase the detector-to-sample distance: because of the isotropic nature of the fluorescence the background will fall off as l^2. However, for light atoms the contribution to the background from fluorescence will be small.

At very short wavelengths (≤ 0.3 Å) Compton scattering becomes the predominant process (Gerstenberg & Hubble, 1982). The Compton scattering has a complex geometrical dependence on the wavelength. [For a detailed study of this effect see, for example, Alexandropoulos & Cooper (1992).] The number of photons scattered at a given angle θ_c rises with this angle from 0 for $\theta_c = 0°$ ('clean miss') to a maximum value for $\theta_c = 180°$. On the other hand, θ_c depends on the energy of the scattered photons, dependent in turn on the wavelength of the incident beam. At long incident wavelengths, the Compton-scattering background will be concentrated at higher angles than at short incident wavelengths. If the detector is moved away from the sample to compensate for the change in wavelength the Compton-background distribution will be the same for all wavelengths (as is the case for Rayleigh scattering). The spectrum of the Compton photons reaching the image plate is too narrow (~ 10 e V) for the variation in the response of the detector (Ito & Amemiya, 1991) to be of any importance.

5. Concluding remarks

We have shown that for the case of a typical stable protein crystal data collection at 0.55 Å does not provide better results than those obtained using a wavelength of 0.92 Å. No overall improvement in the signal-to-background ratio occurred at 0.55 Å wavelength. If the background-to-signal ratio decreased by the inverse square law when the detector was moved back, an improvement by a factor of 2.8 would have occurred at the shorter wavelength. More minor differences are present in the data sets. The background varies in a different manner over the flat image plate at the two wavelengths. For the longer wavelength data there is a lower background at high angles where the data is weak. This geometric effect offers a marginal advantage when using flat detectors. In addition, more data are available for inter-image scaling with the long wavelength data. This is offset by the larger blind region at long wavelengths. The main point is that, with the intensity available at the SRS in Daresbury, it is clearly more advantageous to collect data at 0.9–1.1 Å. At smaller wavelengths the exposure time imposes a penalty (for station 9.5 it takes 7.5 times longer to collect data at $\lambda = 0.55$ Å) which is not balanced by improved quality of the data.

With the high intensities available from third-generation synchrotron sources this major disadvantage will disappear and there will be a wider choice of wavelengths to match any particular experiment. The dominance of Compton scattering at short wavelengths could result in a higher deposition of energy in the crystal giving resultant radiation damage. However the question of radiation sensitivity of the sample is a complex one. It is possible that the onset of damage to the crystal can be slowed down by the use of wavelengths less than 0.9 Å. To prove this more experiments are required.

A. Gonzalez was supported by grants from the Ministerio de Educación y Ciencia and the SERC. We thank T. J. Greenhough for helpful comments on the manuscript.

References

ALEXANDROPOULOS, N. G. & COOPER, M. J. (1992). *International Tables for Crystallography*, Vol. C, edited by A. J. C. WILSON, pp. 574–578. Birmingham: Kynoch Press. (Present distributor Kluwer Academic Publishers, Dordrecht, The Netherlands.)

AMEMIYA, Y. (1990). *Synchrotron Radiat. News*, **3**(2), 21–26.

ARNDT, U. W. (1984). *J. Appl. Cryst.* **17**, 118–119.

CHRISTY, R. W. & PYTTE, A. (1965). *The Structure of Matter*, p. 285. New York: W. A. Benjamin.

GERSTENBERG, H. & HUBBLE, J. H. (1982). *Nuclear Data for Science and Technology*, edited by K. H. BOCKHOFF, p. 1007. Amsterdam: North Holland.

HELLIWELL, J. R. (1992). *Macromolecular Crystallography with Synchrotron Radiation*. Cambridge Univ. Press.

HELLIWELL, J. R., EALICK, S., DOING, P., IRVING, T. & SZEBENYI, M. (1993). *Acta Cryst.* D**49**, 120–128.

ITO, M. & AMEMIYA, Y. (1991). *Nucl. Instrum. Methods*, **310**, 369–372.

OTWINOWSKI, Z. (1991). *DENZO*. Version 0.49. Yale Univ., New Haven, CT, USA.

SERC Daresbury Laboratory (1979). *CCP4. A Suite of Programs for Protein Crystallography*. SERC Daresbury Laboratory, Daresbury, Warrington WA4 4AD, England.

THOMPSON, A. W., HABASH, J., HARROP, S., HELLIWELL, J. R., NAVE, C., ATKINSON, P., HASNAIN, S. S., GLOVER, I. D., MOORE, P. R., HARRIS, N., KINDER, S. & BUFFEY, S. (1992). *Rev. Sci. Instrum.* **63**(1), 1062–1064.